

Magnetic NDT for the Characterization of Industrial Materials

D. K. BHATTACHARYA

National Metallurgical Laboratory, Jamshedpur 831 007

E-mail : dkbhatta@csnml.ren.nic.in

ABSTRACT

Microstructure and residual stresses (RS) are important attributes of an industrial material which determines their various properties. In this paper, first an overview is given on the information available on the relationships of the microstructural parameters and RS on one hand and the parameters related to magnetic hysteresis loop and Barkhausen noise on the other. The relevance of the relationships for microstructural characterisations and RS by magnetic nondestructive evaluation techniques is discussed. Discussion is also made on the development and the use of sensors for the detection and assessment of magnetic flux to characterise microstructures. Two case studies on the use of the techniques in industrial materials and components are presented.

INTRODUCTION

It is well known that microstructures influence material properties - mechanical, chemical and physical. Traditionally, microstructures have been characterized by optical microscopy (OM), scanning electron microscopy (SEM), and transmission electron microscopy (TEM). More recently, acoustic microscopy has been introduced for certain applications in which a knowledge of the substructures is desired. Specialized microscopy techniques such as scanning tunneling microscopy, atomic force microscopy etc. are not yet relevant for general industrial use. OM, SEM, and TEM are normally used on small specimens and in the laboratory. TEM often requires very involved procedures for specimen preparation and complex analysis of data.

Portable optical microscopes are available which can be used on large components. However, they can give only modest magnifications. Replica technique has been developed that can be used for obtaining microstructures from actual components by examining the replicas in optical and scanning electron microscope⁽¹⁾. Possibilities of replica technique for carbide extraction from the sur-

face of an actual component has been indicated in the literature but no actual example is available⁽²⁾. Since the microstructures are strong functions of thermomechanical conditions experienced by a material, and since the thermomechanical conditions may vary from region to region of a component, there is a necessity of the availability of suitable non-destructive test (NDT) techniques which can be used to quickly cover the whole surface and volume of a component without being destructive. While this is the situation which is desired, the use of NDT technique(s) is beset with the problem arising from an absence of well understood relationships with the NDT parameters on the one hand, and the microstructural features on the other.

Magnetic techniques form one of the most important classes of NDT techniques which are used extensively for defect detection/assessment and presently being developed for materials characterizations for component life assessment. They have high sensitivities and simplicity of operation.

Investigations have been carried out on microstructural characterizations using magnetic techniques that can be used for pre-service and in-service applications⁽³⁾

MAGNETIC HYSTERESIS LOOP PARAMETERS

Magnetic hysteresis behaviour in a ferromagnetic (and ferrimagnetic) material is a well known phenomenon which has been extensively discussed in several treatises^(4,5). Figure 1(a) shows the schematic representation of the initial magnetization curve OA and the B-H hysteresis loop ACDEFGA. Figure 1(b) shows a M-H hysteresis loop. The direction of magnetization around the loop is indicated by the arrow. Here B is the induction, M is the intensity of magnetization and H is the applied field strength. They are related through the equation

$$B = M + \mu_0 \cdot H \quad \dots\dots\dots[1]$$

$$B = \mu H, \quad \dots\dots\dots[2],$$

where μ_0 = permeability of vacuum, and μ = permeability of the material.

The occurrence of the magnetic hysteresis is a consequence of the existence of magnetic domains within a ferromagnetic material. The existence of hysteresis implies that irreversible domain related activities take place during magnetization. The domains are regions in which the atomic magnetic spins are oriented in the same directions (direction of spontaneous magnetization). In other words, a domain represents a localized region which is magnetically saturated. For a specimen less than a critical size (10^{-4} to 10^{-5} cm³), no domain wall may exist.

Once this critical size is exceeded, the specimen would divide itself into domains. In a demagnetized state, the directions of spontaneous magnetization in different domains are randomly oriented leading to a small net magnetic field strength which can even be zero. A domain wall is a boundary between two adjoining domains, within which the direction of magnetization gradually changes. In a specimen having domains, the domain configuration will correspond to the lowest energy. Magnetic exchange energy tries to make the domain wall as wide as possible in order to make the angle between adjacent spins within the domain wall as small as possible. The anisotropy energy tries to make the wall thin, in order to reduce the number of spins away from the easy magnetization directions.

Domain wall width of 100nm has been reported for iron⁽⁶⁾. The values of domain wall widths are important with respect to the dimensions of the microstructural features with which the domain walls interact during magnetization processes.

The domain walls can be classified into 180° walls, in which the spins rotate by 180° from one domain to the other, and 90° walls in which the spin rotates by 90° or so. 180° and 90° walls are observed in iron in which the direction of easy magnetization could be any of the six crystallographic directions [100], $[\bar{1}00]$, $[0\bar{1}0]$, [010], $[00\bar{1}]$ and [001]. The domain boundaries between [100] and $[\bar{1}00]$ form 180° domain wall, and those between [100] and [010] form 90° walls. For nickel in which the direction of easy magnetization are $\langle 111 \rangle$ directions, apart from 180° domain wall, 71° and 109° walls are possible. (The angle between $[\bar{1}11]$ and [111] directions in nickel is 71°, and that between [111] and $[\bar{1}\bar{1}\bar{1}]$ is 109°. Often, the 71° and 109° walls are termed as 90° walls because all the three walls are distinguished from the 180° wall with respect to the stress sensitive property. Figure 2 shows the schematic structure of a 180° domain wall. The opposite directions of spontaneous magnetizations on the two sides of the wall are shown. The slowly changing spin direction within the domain wall is also shown.

Figure 1(c) shows the domain activities that take place during the initial magnetization curve [OA in Fig. 1(a)]. The range 'U' is called the range of initial permeability. (Permeability is defined as the ratio B/H). In this range, domain magnetizations in every domain rotate reversibly from the stable directions, and at the same time domain walls are displaced reversibly from their stable positions - the contributions from domain displacements being greater than domain rotation⁽⁴⁾. When the field is increased further, induction B increases rapidly due to irreversible domain wall displacements (of mainly 180° walls). Beyond this range of domain wall displacements, irreversible domain rotation (90° domains) and annihilation takes place.

Beyond this, magnetic saturation approaches where the domain activity becomes reversible again.

The domain activities during the course of hysteresis ACDE [see Fig. 1(a)] are shown schematically in Fig. 1(d). When the magnetic field is reduced below the range of magnetic saturation, domain nucleation starts followed by irreversible domain displacements, domain rotation, and annihilation, and lastly reversible domain rotation.

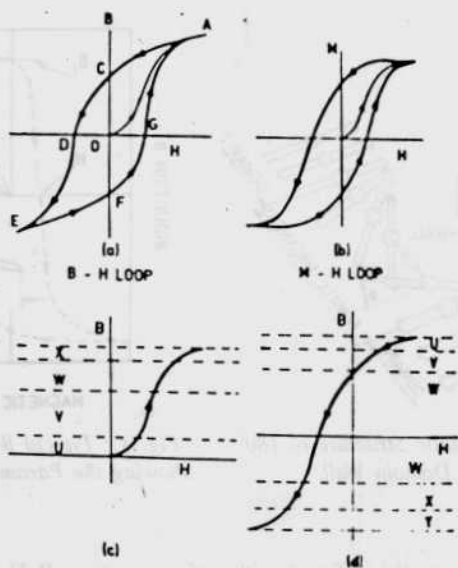


Fig. 1(a) and (b) : Schematic Sketch showing Magnetization through Hysteresis Loops.; (c) Magnetization Process along Initial Magnetization curve OA of fig. (a) 'U' = Initial Permeability Region 'V' = Irreversible Domain Wall Displacements, 'W' = Irreversible domain rotation and annihilations, 'X' = Approach to Saturation.; (d) Magnetization Processes during a Half Hysteresis Sweep: 'U' = Reversible rotation of magnetic moments. 'V' = Domain nucleations. 'W' = Irreversible Domain Wall Displacements. 'X' = Irreversible Domain Rotation and Annihilations. 'Y' = Approach to Saturation.

The domain related activities have been characterized by both theoretical analysis and experimental investigations. The theoretical analyses have been aided by experimental observations of domain wall nucleations by Bitter technique in specially prepared single crystal of iron in which the roles of surface imperfections and inclusions have been studied⁽⁷⁾. The domain wall displacements that follow the domain nucleation have been analyzed theoretically and investigated experimentally. The nature of the domain wall motion controls the coercivity of a material, an important material property⁽⁸⁾.

Figure 3 shows the parameters that can be derived from a hysteresis loop and which can be used for characterizing microstructural features and mechanical behaviour of materials. The parameters are: B_r = retentivity; H_c = Coercivity; μ_i = Initial permeability; μ_m = Maximum permeability; μ_Δ = Incremental permeability. Besides these, it is possible to use maximum differential permeability (dB/dH_{max}) which is the maximum slope of B-H hysteresis loop. A discussion on the importance of the parameters and their applicability is given below.

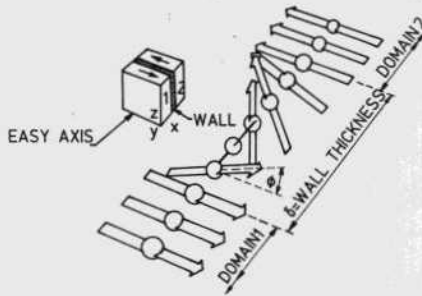


Fig. 2 : Schematic Structure of 180 Degree Domain Wall.

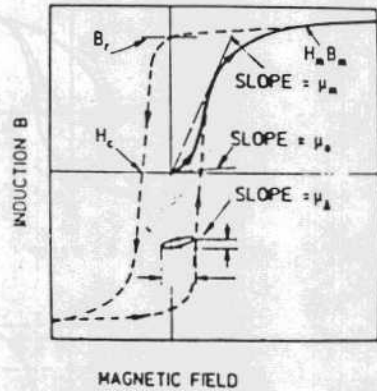


Fig. 3 : Typical B-H Hysteresis Loops showing the Parameters derived from it.

COERCIVITY

Coercivity is normally defined with reference to a B-H loop in which the specimen has been taken to saturation, as the magnetic field strength corresponding to the zero value of B [Fig. 3]. Coercivity has been found to be highly sensitive to the microstructure and stress conditions in a material.

Coercivity and Material Hardness

A large number of investigations have been reported on the relationship of magnetic hardness (given by coercivity) and metallurgical hardness⁽⁹⁻¹¹⁾. Figure 4 shows the direct and approximately linear relationship between coercivity and hardness of pearlitic steels. Such relationships prompt one to consider coercivity as a monitoring parameter of the metallurgical state of a ferromagnetic steel or an alloy. Metallurgical hardness is the manifestation of the synergistic effect of a large number of variables such as matrix hardness (solid solution hardening), dislocation density, internal strain, size/shape/volume of secondary phase precipitates, the nature of the interfaces between the precipitates and matrix, porosities, grain size, etc. Most of these microstructural fea-

tures also influence the coercivity. However, the effect of the microstructural features on the metallurgical hardness may be entirely different from those on coercivity. For example, a secondary phase may be soft in terms of metallurgical hardness, but due to its magnetic anisotropy (with respect to the matrix) or due to its non-ferromagnetic nature, may act as strong pinning points to the domain wall, aiding to the magnetic hardness. Therefore, linear and direct relation between coercivity and metallurgical hardness may be only one of the ways that these two parameters may be related. Another important reason due to which deviation from linearity may be expected is the precipitate size influencing the domain activities such as domain nucleation and domain wall motion.

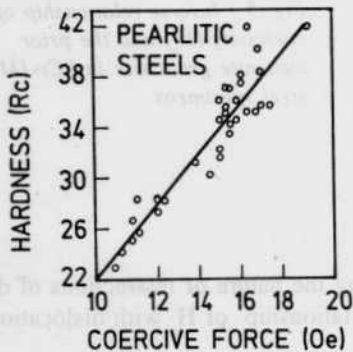


Fig. 4 : Relation between Material Hardness and Coercivity in Pearlitic Rail Steel⁽¹¹⁾

Coercivity and Mechanical Properties other than Hardness

The functional relationship between coercivity on the one hand and hardness/dislocation density/grain size on the other indicate that coercivity should be a function of mechanical properties other than hardness. Hardness is known to be related to other mechanical properties like ultimate tensile strength, yield strength, creep properties etc. Therefore, relationship of coercivity with these parameters can be expected⁽¹²⁾.

Coercivity and grain size

Experimentally, the inverse relationship between coercivity H_c and average grain size d' has been found to be valid for pure iron and low carbon steel and alloy steel⁽¹³⁾.

$$H_c = k_1 \cdot d'^{-1} + k_2 \quad \dots[5]$$

in which k_1 and k_2 are constants

For a two phase pearlite - ferrite steel the following equation has been found to be valid⁽¹⁴⁾.

$$H_c = k_1 \cdot C_f/d_f + k_2 \cdot C_p/d_p \quad \dots[6]$$

where c_f and c_p are the fractions of ferrite and pearlite; d_f and d_p are the average sizes of the ferrite and pearlite grains respectively.

Figure 5 shows the inverse relationship of coercivity and prior austenite grain sizes in 9Cr-1Mo steel specimens austenitized at various temperatures before water quenching to get martensite microstructures.

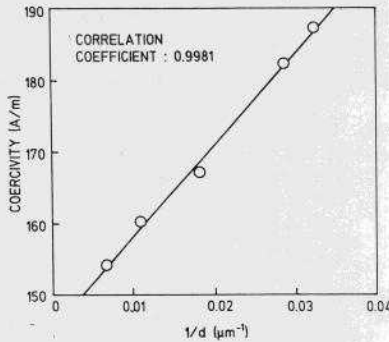


Fig. 5 : Inverse relationship of coercivity (H_c) and the prior austenite grain size in 9Cr-1Mo steel specimens

Coercivity and dislocation density

Various theoretical approaches regarding the nature of interactions of domain walls with dislocations have given a relationship of H_c with dislocation density of the following common type⁽⁹⁾

$$H_c \propto N^{1/2} \quad \dots[9]$$

where, N = Dislocation density.

Higher dislocation densities are associated with large plastic deformation which often lead to texture that may affect the magnetization behaviour considerably. Again, the energy of interaction of a dislocation with domain wall would change when secondary phase precipitates are pinned by the dislocations. It may then be difficult to differentiate the contribution of the dislocation per se and the dislocations associated with pinned precipitates.

Coercivity and Secondary Phase Precipitates

A secondary phase particle is one of the most important microstructural features which influences the coercivity. Besides the size of the precipitates, other factors affecting coercivity are the volume of the precipitate relative to the matrix and their spatial dispersion. A relationship between H_c and V (volume fraction of the precipitates) of the type as given below has been proposed.

$$H_c = p \cdot k \cdot V^n / M^s \quad \dots[10]$$

where p = dispersion factor, k = anisotropy constant, V = volume of inclusions, n is an exponent whose value depends on the shape of the particle.

Coercivity and other Hysteresis Loop Parameters

Functional relationship between coercivity and other parameters derived from magnetic hysteresis loops such as initial permeability, maximum permeability, remanence (retentivity) etc. have been found. It is not surprising since all of these parameters are related to various types of domain activities that take place during magnetic hysteresis.

Coercivity and other metallurgical parameters.

Coercivity is affected in varying degrees by solid solution hardening, plastic deformation, internal stresses, shape anisotropy, crystal anisotropy and temperature. Plastic deformation on a material imparts one or more of the following - increase in dislocation density, generation of internal stresses, generation of texture (strain anisotropy), and stress induced phase transformation.

BARKHAUSEN NOISE ANALYSIS

There are two types of Barkhausen noise signals: (a) Magnetic and (b) Acoustic. Magnetic Barkhausen Noise (MBN).

MBN signals are generated when a ferromagnetic (or a ferrimagnetic) material is magnetized through a hysteresis loop. The source mechanism of this type of signals is mainly the motion of 180° domain walls from one pinning point to another, which changes the local magnetic moment. These signals can be sensed by a sensor coil or an audio head.

MBN discovered by Barkhausen⁽¹⁵⁾ was the first experimental proof of the existence of domain walls. The term "noise" was coined because the existence of signal was discovered in the form of a crackling noise in a telephone speaker. Fig. 6 shows a copy of the original Figure published by Barkhausen showing the schematic experimental set up. 'E' was a ferromagnetic core (iron and steel), S' a search coil with 300 turns and having a diameter of 25 mm, T' a telephone, 'V' a 10,000 fold amplifier (term used by Barkhausen; it is equal to 80dB), G' a damped galvanometer, and M' a hand held magnet. When the magnet was moved towards the specimen, galvanometer deflection and generation of sound in the telephone speaker took place simultaneously.

Important observations made by Barkhausen are given below together with comments based on the understanding on MBN signals that we have today. The latter are given within brackets.

- (a). The noise was audible.
- (b). When the magnetic field was varied, the noise was found to be absent in certain range of the variation. (Noise is mainly emitted when the ratio dB/dH is maximum).

- (c). Thicker core gave weaker noise. (due to eddy current damping).
- (d). Stronger noise was heard when the steel was milder. Hardened steel did not give any noise at all. (Less MBN signals in hardened steel due to the presence of internal stress.)

Barkhausen predicted that this phenomenon had a potential for use as an inspection technique.

Indeed, it is now a very important nondestructive tool for the characterization of microstructure and residual stress.

From the time of discovery of the MBN to this day, the instrumentation has improved in line with the development in the electrical and electronics science and engineering, and the signal analysis technique. However, the basic modules are the same, namely (a) a varying magnetic field, (b) sensor for sensing and acquiring the discontinuous magnetic signal, (c) a display of the signal in suitable forms and, (d) analysis of the signal.

Figure 7 shows the block diagram of a MBN equipment. Though MBN was discovered through acoustic signal (crackling sound in telephone) this signal was only a converted signal. A true acoustic signal (elastic wave) is also generated in a ferro-magnetic (or a ferrimagnetic) material when the induced magnetic field inside a specimen is varied. This phenomenon was discovered by A.Lord⁽¹⁶⁾.

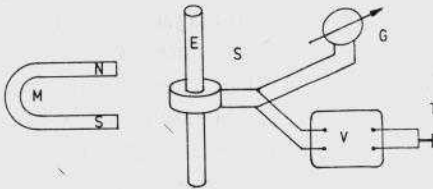


Fig. 6 : Copy of Schematic Sketch of the Experimental Set Up used by Barkhausen¹⁵

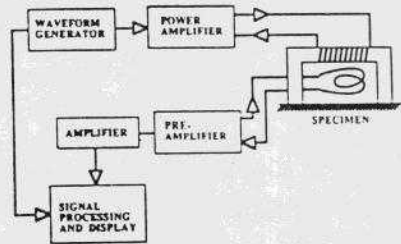


Fig. 7: Block Diagram of a Typical Magnetic Barkhausen Noise Analysis System.

Figure 8 shows the B-H hysteresis loop of a 17-4PH stainless steel specimen. Superimposed on this Figure is the rms voltage distribution of MBN signals. The positioning of the MBN peak corresponding to the coercivity point (where dB/dH is maximum) can be seen.

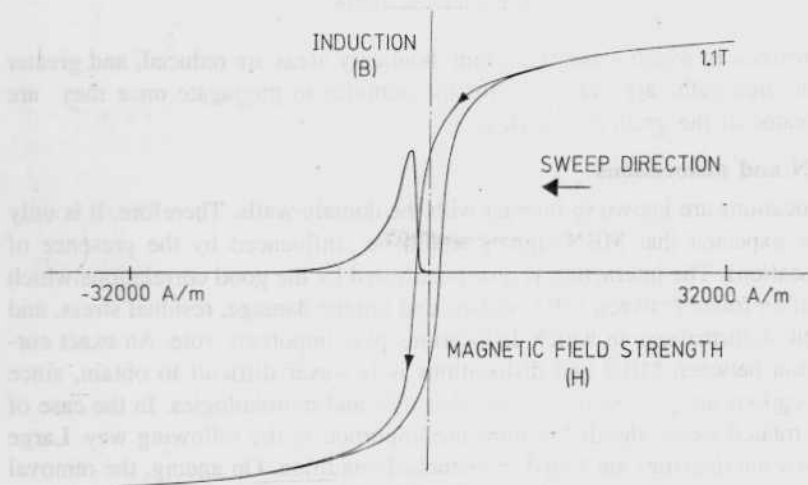


Fig. 8 : A B-H Hysteresis Loop of a 17-4PH Martensitic Stainless Steel Specimen. A Magnetic Barkhausen Noise rms Voltage Plot is Superimposed for a half hysteresis sweep.

The phenomenon of eddy current damping during MBN signal generation, which makes the MBN analysis technique applicable only to the surface region of a specimen, was observed by Bozorth⁽¹⁶⁾

MBN and microstructure

MBN is a strong function of secondary phases, grain size, dislocation structure, and locked in macro/micro stresses, which are the principal features of a microstructure. Several reviews on MBN are available which include the discussion on all or some of these features⁽¹⁸⁻²⁰⁾

In the eighties and nineties and to date, several reports on the use of MBN analysis for characterizing microstructure of heat treated steels have been published.

MBN and grain size

Apart from the secondary phase precipitates, the other microstructural features of importance to MBN analysis are grain size and dislocation density and distribution. Considering that in many cases, the maximum in MBN signal intensity occurs around the point of coercivity where the ratio dB/dH ratio is maximum, it is reasonable to expect that MBN signal should have a correlation with grain size; because, it has been seen by both theoretical analysis and by experimental observations, that coercivity has an inverse relationship with grain size. This relationship comes because the domain wall impediment is more important than domain wall nucleation. On the basis of similar argument, it may be said that MBN signal peak heights should increase with higher

grain sizes, in which case, the grain boundary areas are reduced, and greater mean free paths are available for the domains to propagate once they are nucleated at the grain boundaries.

MBN and dislocations

Dislocations are known to interact with the domain walls. Therefore, it is only to be expected that MBN signals would be influenced by the presence of dislocations. The interaction is also manifested by the good correlations which are often found between MBN signals and fatigue damage, residual stress, and plastic deformations in which dislocations play important role. An exact correlation between MBN and dislocations is however difficult to obtain, since dislocations are present in varying densities and morphologies. In the case of heat treated steels, the dislocations are important in the following way. Large dislocation densities are found in quenched condition. On ageing, the removal of the macrostresses may change the dislocation morphology; this is countered, if fine sized precipitates are formed and are well distributed in the matrix. The dislocation morphologies would, however, change if after prolonged thermal ageing, recovery and recrystallization take place in the matrix. If the dislocations are associated with other microstructural features such as secondary phase precipitates, grain boundaries etc., then it is all the more difficult to obtain an idea of the influence only from the dislocations.

Acoustic Barkhausen Noise (ABN)

Acoustic Barkhausen Noise (ABN) signals are elastic waves generated during a hysteresis sweep in a ferromagnetic (or a ferrimagnetic) material. These signals are also known as magnetomechanical acoustic emission (MAE). The source mechanism of ABN is considered to be the motion of 90° domain walls, and possibly the rotation of vector of spontaneous magnetization. These two processes give rise to elastic distortion owing to the magnetostrictive properties of ferromagnetic (and ferrimagnetic) materials. The magnetostrictive properties of materials as being the main reason for ABN generation has been questioned on the basis of work in ferrimagnetic materials such as ferrites, and instead, ABN has been attributed to be due to domain nucleation and annihilation.

ABN has been found to be highly sensitive to the presence of internal stresses, and therefore ABN analysis has been found to be an important technique for residual stress measurements. Less emphasis has been given to find the applicability of ABN for microstructural characterizations. However, the available results on microstructural characterization are promising.

Importance of ABN for microstructural characterizations.

ABN differs from MBN signals in several ways. First, the source mechanisms

are different. Secondly, ABN is an elastic wave, and therefore, its amplitude is not affected by eddy current damping, which is important for MBN signals. Therefore, signals averaged over a larger volume as compared to those relevant for MBN, is obtained. In view of the differences in the ABN and MBN signals as mentioned above, it is important that the work on microstructural characterizations be done by using both MBN and ABN analysis. Another important point about ABN is that the signals are much weaker as compared to the MBN signals and therefore requires much greater amplifications.

MAGNETIC TECHNIQUES FOR RESIDUAL STRESS MEASUREMENTS

Residual Stress (RS) can be defined as the locked-in stresses present in a free body (under a uniform temperature), i.e. in a body in which no external load is applied. If an external load is present, stresses due to this load is superimposed on the existing RS patterns.

RS is generated whenever there are non-uniform plastic deformations, and/or chemical changes within a body either during fabrication or during service. Non-uniform plastic deformations may take place by thermal and mechanical effects such as those experienced during welding, casting, heat-treatment etc. There is, in fact, no industrial process that does not generate RS and there is no stress relief operation that removes RS entirely. The importance of the studies on RS comes from the uncertain nature of the RS patterns that are present after a component is fabricated, and the effect of RS on the performance of a component. RS has been found to be an important parameter for the assessment and characterisation of fatigue damage before and after the initiation of micro/macrocra^{cks}^(21,22).

Magnetic Hysteresis Loop Parameters and Stress

The application of an external load on a ferromagnetic material changes the magnetic hysteresis loop^(4, 5). The changes are manifested in the slope of the loop, area within the loop, contour around the region of the coercivity point and the knee regions. It is also seen that the shape changes depend on whether the induction is measured parallel to the stress or perpendicular to it. These phenomena of shape changes of hysteresis loops are indicative of the changes in the dynamics of magnetic domains due to the changes in micro-structural and sub-structural features that are brought about by the application of a load, cold work and RS. The stress has a great effect on magnetic hysteresis because of reverse magnetostrictive effect^(4,5). Magnetostriction is defined as the change in the dimensions of a ferromagnetic (or ferrimagnetic) specimen when a magnetic field is applied through the specimen. Reverse magnetostriction is the effect of load and stress on the magnetic process.

Hysteresis parameters such as coercivity and differential permeability^(23,24) - two important hysteresis parameters have been related to stress.

Barkhausen Noise Signal and Stress

As already indicated, magnetic Barkhausen noise (MBN) is associated with eddy current effect. Therefore, such signals generated at the interior of a specimen is exponentially attenuated and only the signals from the surface regions are sensed. Unlike MBN, acoustic Barkhausen noise (ABN) is not a surface specific signal since it is an acoustic signal and is not subjected to an eddy current effect like MBN. Acoustic Emission probes with resonant frequencies of 175 kHz has been used with success⁽²⁵⁾. 175 kHz is a low frequency signal for which it would not be significantly attenuated while in passage through a specimen. Therefore, ABN gives an averaged information from a material volume that is interrogated by the applied magnetic field. By changing the frequency of magnetic sweep, the material volume from which ABN is generated can be varied. Higher the frequency of magnetic sweep more eddy current or skin effect comes into play making the signal more and more surface specific. Higher frequency also facilitates the generation of ABN signals of greater intensity and energy. ABN signals as detected are normally weaker than MBN.

CASE STUDIES

Case 1

The material under a failure investigation was shot peened suspension spring which had failed during service in an automobile. The diameter of the spring rod was 10 mm and the spring rod section under study was part of a spring having diameter of ~80 mm. The spring material was a medium carbon steel (C-0.57, Mn-0.82, Si-1.83 in wt%), the schematic representation of spring section is presented in Fig. 9. Visual observation showed that the crack started from the inner diameter of the spring and extended to the outer surface.

MBN measurements at a magnetizing frequency of 120Hz were taken at four different circumferential positions 12-, 3-, 6-, and 9- O'clock position facing the failed end, and various axial positions which were 1 cm apart from the fail end as shown in Fig. 9(a). Residual stress was also measured by X-ray diffraction (XRD) from the outer surface (12 O'clock) to the inner surface surface 6 O'clock) along the cross section of the spring as shown in Fig. 9(b). Fig.10 shows the rms voltage of MBE signal at four circumferential positions and different axial positions of the spring section. Residual stress as determined by XRD is shown in Fig. 11.

The MBN activity at 12 O'clock position was found to be higher than in the 6 O'clock position. Since MBN activity decreases with the increase of com-

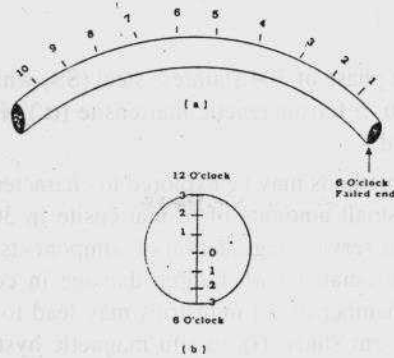


Fig. 9. (a) : Schematic presentation of the shot peened spring showing different points (1 to 10) where MBN measurements were done and (b). cross sectional view of spring rod section showing different points where X-ray Diffraction measurements were done.

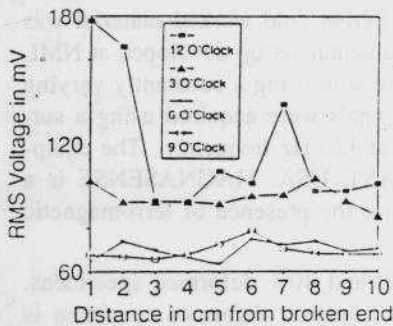


Fig. 10 : RMS voltage of MBN signals at different positions of spring rod section.

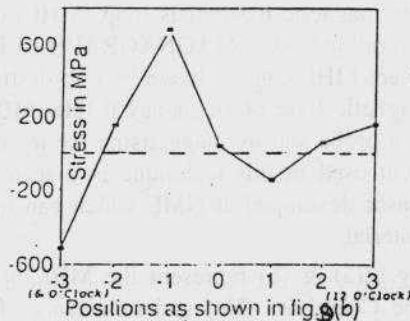


Fig. 11 : Residual stress measured by XRD at different positions of the spring rod cross section as shown in Fig. 9.

pressive stress in steel, the MBN study in the present case indicates that the compressive stress at the inner diameter (i.e. the arc covering 3-6-9- O'clock positions), of the spring section was higher than the outer one (9-12-3- O'clock positions). XRD results also corroborated the MBN results in the sense that the compressive stress in 6 O'clock position was higher than the 12 O'clock position. XRD also indicated the existence of high tensile stressed (~ 700 MPa) region at the subsurface close to the inner surface of the spring section where the compressive stresses were maximum.

Microstructural investigation revealed that the material was tempered martensite with high ratings of oxide inclusions. The existence of excess inclusions made the materials inherently bad against fatigue damage. It appears that the nonuniform distribution of the compressive stress in the service exposed spring section and the presence of high tensile stress at the subsurface near the inner diameter initiated the cracks in the interface of the inclusions and matrix.

Case 2

A part of the austenite phase of 304 stainless steel (SS) which is non ferromagnetic is transformed to a ferromagnetic martensite (α') phase when the steel is plastically deformed.

Therefore, magnetic methods may be explored to characterise the cold worked 304SS. Detection of small amounts of α' -martensite in 304SS is very useful for the evaluation of in-service degradation of components. For example, local plastic deformation associated with fatigue damage in components made of 304SS like Plenum chamber of oil industries may lead to precipitation of α' -martensite. In the present study, (i). in-situ magnetic hysteresis loop (MHL), (ii). MBN analysis, and (iii). MANGNASENSE - a magnetic sensor developed at National Metallurgical Laboratory have been used to study the presence of α' -martensite phase in cold worked 304 stainless steel.

The magnetic hysteresis loop (MHL) of different cold worked material was determined using MAGNAGRAPH-an instrumental set-up developed at NML where MHL can be drawn by non-destructive way using a constantly varying magnetic field of frequency 0.1Hz. MBN signals were acquired using a surface probe and by magnetising the material at 120 Hz frequency. The equipment used in this technique is μ -scan by AST, USA. MAGNASENSE is a sensor developed at NML which can measure the presence of ferromagnetic material

Fig.12(a) & (b) represent the MHL of 20% and 40% deformed specimens. The Coercivity (H_c) and remanence (B_c) of various deformed specimen is shown in Fig. 13. The Coercivity and remanence increased with the percentage of deformation. Fig. 14 represents the dependence of RMS voltage of MBN signal with magnetising field of different degrees of cold worked specimens. Barkhausen activity increases with the degree of cold working which is expected as the amount of α' -phase and hence the number of domains increase with deformation.

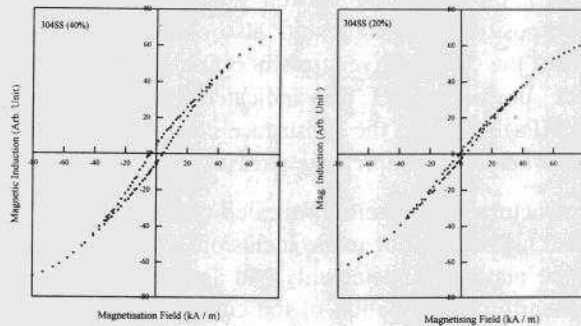


Fig. 12 : Magnetic hysteresis loop of (a) 20% cold worked and (b) 40% cold worked 304SS

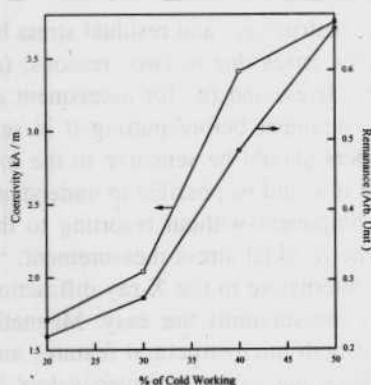


Fig. 13. Variation of H_c and B_r with the percentage of deformation in 304SS

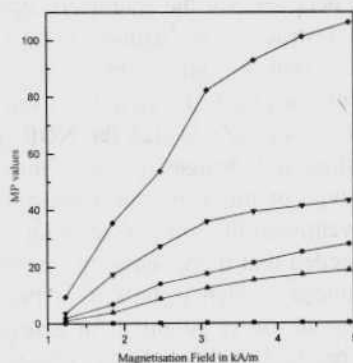


Fig. 14: Variation of MBN signal voltage with magnetisation field strengths for cold worked 304SS.

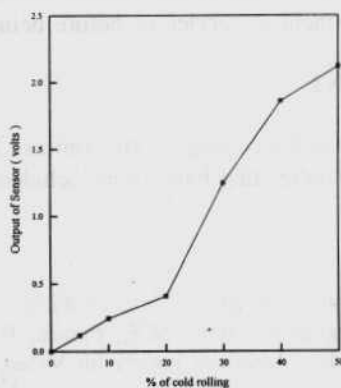


Fig. 15. Output response of Magnetic sensor (MAGNASENSE) as a function of cold working in 304SS.

The results of MANGANESE have been plotted in Figure 15 which indicates that the sensor output voltage increases linearly at the beginning of deformation. Rapid increase in output voltage observed at the intermediate range of deformation and the output voltage tends to saturate at higher degree of deformation. It is interesting to note that the MANGANESE is sensitive even for 5% deformation of 304SS.

CONCLUSIONS

The necessity for the characterisation of microstructures and residual stress by non-destructive evaluation (NDE) techniques arises due to two reasons: (a) for assessment and extension of component lives, and (b) for assessment of thermo-mechanical treatment given in a component before putting it in service. It is desirable that the NDE parameters should be sensitive to the microstructural changes in such a manner that it would be possible to understand the type of microstructures present in a component without resorting to the conventional microscopy techniques. For the residual stress measurement, it is needed that there should be techniques alternative to the X-ray diffraction technique (which is bulky) so that in-situ measurements are easy. Magnetic techniques offer potential for assessment of both microstructural features and the residual stresses. Major efforts have been put by many investigators to develop them for the characterisation of microstructures and residual stresses.

The overview has shown that the magnetic parameters related to hysteresis loop and Barkhausen noise are sensitive to the microstructural parameters and residual stress. The relationships are, however, not always straightforward. Therefore, careful laboratory studies are needed before a technique can be used on an actual component in service or before being put in service.

ACKNOWLEDGEMENT

The author wishes to thank his colleagues Dr. Amitava Mitra and Ms. S. Palit Sagar for the two case studies that have been included in the paper.

REFERENCES

1. Sullivan, E.V. Microstructural Science. Vol. 15. Field Metallography, Failure Analysis, and Metallography. (Blum, M.E., French, P.M., Middleton R., and Vander Voort, G.F, eds). American Society for Metals. pp 3-12. (1987).
2. Viswanathan, R. Damage Mechanisms and Life Assessment of High Temperature Components, ASM International, Metals Park, OH, USA. (1989).
3. Hildebrandt, U.W, and Schneider, K. Determination of Residual Life of Turbine Components. Report COST-501-D29. ASEA Brown Boveri Aktiengesellschaft, Mannheim, Switzerland. (1988).
4. Chikazumi S. Physics of Magnetism. John Wiley and Sons Inc. New York. (1964)
5. Cullity B.D. Introduction to Magnetic Materials. Addison Wesley Publishing Co. Reading, Massachusetts, USA. (1972).
6. Kerr, J., and Wert, C. J. Appl. Phys 26 (1955) 1147 - 1151.

7. Bates L.F., and Martin D.H. Proc. Phys. Soc. (London). 69 (1956) 145-152. 18. Nix, William D., and Huggins, Robert A. Phys. Rev. 135 (1964) A401-A407.
8. Nix, W.D., and Huggins, R.D, Phys. Rev, 135, A401-A407 (1964)
9. Mikheev, M.N., and Gorkunov, E.S. Sov. J. NDT, 21 (1985) 155 - 172.
10. Bussiere, J.B., Mat Eval. 44 (1986) 560 - 567.
11. Bussiere, J.B. Applications of NDE to the processing of Metals, in "Review of Progress in Quantitative Non- destructive Evaluation". Vol. 6B. (Thompson, D.O., and Chimenti, D.E.eds.) Plenum Press. New York. (1987).
12. Tanner, B.K., Szpunar, J.A., Wilcock, S.N.M., Morgan, L.L., and Mundell, P.A., J. Mat. Sc., 23 (1988) 4534 - 4540
13. Ranjan, R., Buck, O., and Thompson, R.B. Review on Progress in Quantitative Non-destructive Evaluation (Thompson, D.O., and Chimenti, D.E.eds) Vol. 5B. Plenum Press. pp1335-1344 (1986).
14. Wilcock, S.N.M., Tanner, B.K., and Mundell, P.A. J. Mag. Magn. Mat., 66 (1987) 153-157.
15. Barkhausen, H., Physik. Zeitschr. 20 (1919) 401-402.
16. Lord, A.E. jr. Physical Acoustics Vol.XI (Mason, W.P. and Thurston. R.N.) Academic Press, New York. pp 290-345 (1975).
17. Bozorth, R.M., Phys. Rev. 39 (1932) 353 - 356
18. Rudyak, V.M., Soviet Phys. 13 (1971) 461-47
19. Matzkanin, G. A., Beissner, R.E., and Teller, C.M. Report NTIAC-79-2. Nondestructive Testing Information Centre, Southwest Research Institute, SA, Texas, USA (1979).
20. Lomaev. G.V., Malyshev, V.S., and Degterev, A.P., Sov. J. NDT, 21 (1985) 189-203.
21. Field, J.L., Behnaz, F., and Pangborn, R.N. Fatigue Mechanisms : Advances in Quantitative Measurement of Physical Damage, ASTM - STP 811, Lankford, J., Davidson, D.L., Morris, W.L., Wei, R.P. eds. American Society for Testing and Evaluation. pp 71-94 (1983).
22. Karjanainen, L.P., Moianen., and Raotioaho, R., Mater. Eval. pp 45-51 (1979)
23. Atherton, D.L., Welbourn, C., Jiles, D.C., Reynolds, L., and Scott-Thomas, IEEE Transactions on Magnetics, Vol Mag-20, 2129-2136 (1984).
24. Mushakin, S.A., Novikov, V.F., Borsenko, V.N. Sov. J. of NDT, pp. 633-638. (1988).
25. Shibata, M., Kobayashi, E., and Ono, K, J. Acoustic Emission. 4, 93-101 (1985).